Anal Bioanal Chem (2012) 402:1269–1276
DOI 10.1007/s00216-011-5531-0

ORIGINAL PAPER

Characterization of sodium hyaluronate blends using frit inlet asymmetrical flow field-flow fractionation and multiangle light scattering

Muhammad Ali · Euijin Hwang · Il-Hwan Cho · Myeong Hee Moon

Received: 31 May 2011 / Revised: 20 October 2011 / Accepted: 23 October 2011 / Published online: 20 November 2011

Abstract We characterized ultrahigh molecular weight sodium hyaluronate (NaHA) and blended pharmaceutical products containing NaHA using flow field-flow fractionation and multiangle light scattering–differential refractive index (FlFFF-MALS-DRI). NaHA is a water-soluble polysaccharide with a range of molecular weights (MW: 10^5~10^8 Da) that is found in body fluids and tissues. NaHA is also used commercially in pharmaceutical and cosmetic applications. We used a frit inlet asymmetrical FlFFF channel to separate aqueous polymers according to their hydrodynamic size, and we used on-line measurements of light scattering to obtain the MW distribution (MWD) as well as structural information about NaHA in aqueous solution. In this study, we investigated NaHA and anti-adhesive blend mixtures of NaHA (a commercial NaHA blend mixture containing sodium carboxymethyl cellulose and a new blend with hydroxyethyl starch (HES)) to determine the molecular weight distribution MWD of NaHA and the blend mixtures and to obtain structural information about these compounds in aqueous solution. We also examined the characteristics of NaHA–HES–polylactic-*co*-glycolic acid film products exposed to gamma radiation for sterilization purposes.

Keywords Flow field-flow fractionation · Multiangle light scattering · Sodium hyaluronate (NaHA) · NaHA blend mixtures

Electronic supplementary material The online version of this article (doi:10.1007/s00216-011-5531-0) contains supplementary material, which is available to authorized users.

M. Ali · M. H. Moon (✉)
Department of Chemistry, Yonsei University,
Seoul 120-749, South Korea
e-mail: mhmoon@yonsei.ac.kr

E. Hwang · I.-H. Cho
Department of Biotechnology,
Shinpoong Pharmaceutical, Co. Ltd,
Ansan, Kyeonggi-Do 748-31, South Korea

Introduction

Sodium hyaluronate (NaHA) or the sodium salt of hyaluronic acid is an ultrahigh molecular weight (MW) water-soluble polymer found in skin, synovial fluid, human cartilage, and rooster combs, among various biological sources [1–4]. NaHA is a polysaccharide composed of a repeating disaccharide unit of D-glucuronic acid and *N*-acetyl-D-glucosamine. Due to the viscoelastic and water-absorbing properties of NaHA, it is currently used as a replacement material for vitreous humors, in joint lubrication, and in cosmetic applications [2, 5, 6]. NaHA is utilized as an anti-adhesive agent during surgery; for this purpose, it is prepared as a blend mixture of NaHA and low molecular weight sodium carboxymethyl cellulose (NaCMC) in solution [7, 8]. NaHA-based anti-adhesives are either of the membrane or gel type; the latter conforms to a film when applied to internal organs during surgery. Because NaHA is enzymatically degraded in the human body in 1–3 days, during which time it reduces adhesion by inhibiting fibrin formation [9], NaCMC, which is not degraded in the human body, is mixed with NaHA [7]. Hydroxyethyl starch (HES) is an alternative material that can be blended with NaHA due to its biodegradability. HES is a water-soluble semi-synthetic polysaccharide modified from amylopectin, the short-chain branch component of starch [10]. HES is obtained by reacting starch with a higher content of amylopectin with ethylene oxide to replace the hydroxyl groups of the anhydroglucose units by hydroxyethyl groups. Hydrox-

yethylation hampers enzymatic biodegradation of HES *in vivo* and has allowed it to be used as a plasma volume expander [10, 11]. Therefore, HES increases the solubility, solution stability, and *in vivo* half-life of NaHA when blended with it. This blend could also potentially be used as a surgical anti-adhesive material.

The MW and MW distribution (MWD) of polysaccharides are usually determined using size exclusion chromatography (SEC) coupled with viscometry or multiangle light scattering (MALS). However, ultrahigh MW polymers often exceed the separation capabilities of SEC because of the lack of packing materials with sufficiently large pore sizes to accommodate ultrahigh MW species, the possible degradation of polymers by shear, and a lack of appropriate calibration standards. For ultrahigh MW NaHA, it was reported that shear degradation can occur for molecules larger than three million Da [12]. Flow field-flow fractionation (FlFFF) is an alternative method that can be used to separate and characterize ultra-large molecules when it is employed together with MALS. FlFFF is an elution-based separation technique that has been used to characterize particulate materials, polymers, and biological macromolecules including proteins, DNA, and cells [13–16]. Separation in FlFFF is carried out in a flat, open channel space by using a migration flow and crossflow stream that moves across the channel in a perpendicular direction to the migration flow; the order of elution in FlFFF is typically based on an increase in the hydrodynamic diameter. FlFFF-MALS has been used to separate and characterize various water-soluble polymers including polysaccharides [17], celluloses [18, 19], k-carageenan [20], polyacrylamide [21], amylopectin [22, 23], and NaHA [24–26]. In particular, frit inlet asymmetrical FlFFF (or FI-AFlFFF) has been shown to be able to separate ultrahigh MW NaHA materials (10^5~10^8 Da) and their degraded products [24, 27, 28]. Because a FI-AFlFFF channel operates without the requirement for a focusing/relaxation procedure, in which migration flow is temporarily halted for sample relaxation, it can be used to characterize ultrahigh MW polymeric materials.

In this study, we used FI-AFlFFF-MALS to study NaHA–HES blend mixtures that have the potential to function as anti-adhesives. We used research-grade NaHA materials to confirm the performance of the FI-AFlFFF-MALS system in terms of separation and MWD characterization. The molecular weight distribution and molecular conformation of a raw NaHA material blended with HES (NaHA–HES) and a commercial anti-adhesive product (NaHA–NaCMC) were compared. We also examined whether gamma radiation of NaHA–HES–polylactic-*co*-glycolic acid (PLGA) film for sterilization purposes changed the MWD and structure of the film.

Experimental

Materials and reagents

The two research-grade NaHA materials (MW, 2.344×10^5 and 7.80×10^5 Da from SEC-MALS) were obtained from Lifecore Biomedical, LLC (Chaska, MN, USA) and a commercial NaHA material was purchased from Shandong Freda Biopharm Co, Ltd. (Jinan, China). Raw NaHA was extracted from *Streptococcus* by Shinpoong Pharmaceutical Company, Ltd. (Ansan, Korea). The HES sample was obtained from Fresenius Kabi Austria GmbH (Linz, Austria) and the weight average molecular weight (Mw) of the HES sample was 670 kDa (0.75 molar substitution level) according to the manufacturer. The crosslinked NaHA–HES sample was prepared by Shinpoong at a concentration of 1% NaHA with 0.5% HES in equal volumes. The NaHA–NaCMC sample was Guardix-sol, a commercial product produced by Hanmi Pharm. Co. Ltd (Seoul, Korea). NaHA–HES–PLGA film products were prepared by Shinpoong and sterilized by gamma irradiation at radiation dosages of 15.0 and 40.0 kGy. To analyze the NaHA–HES–PLGA mixture, the film layer was dissolved in 0.1 M $NaNO_3$ solution first and then the insoluble PLGA particles were removed by centrifugation at 8,550 g for

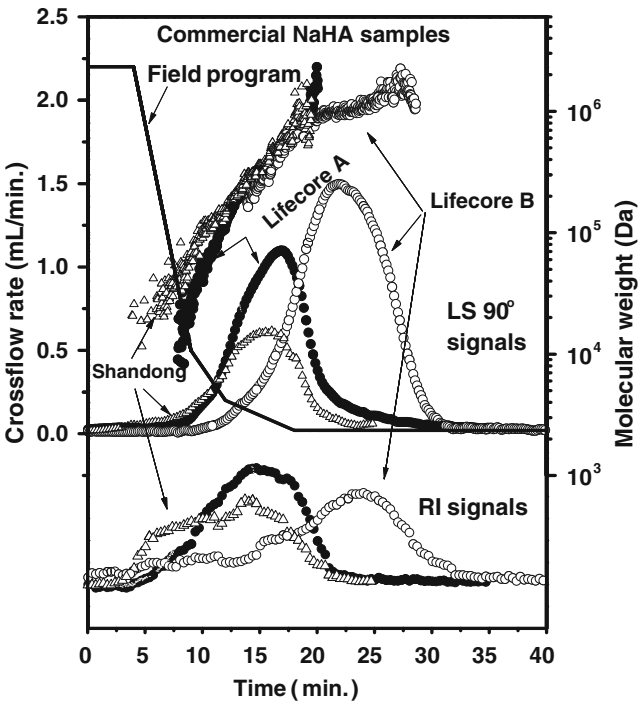

Fig. 1 FI-AFlFFF-MALS fractograms of the three commercial NaHA products, and the calculated MW values obtained at an outflow rate of 0.1 mL/min and a crossflow rate programming condition marked as a straight line (crossflow rate maintained at 2.2 mL/min for 4 min, started decaying linearly to 0.5 mL/min for 5 min, to 0.2 mL/min for 3 min, to 0.02 mL/min for 6 min, and then maintained for 22 min)

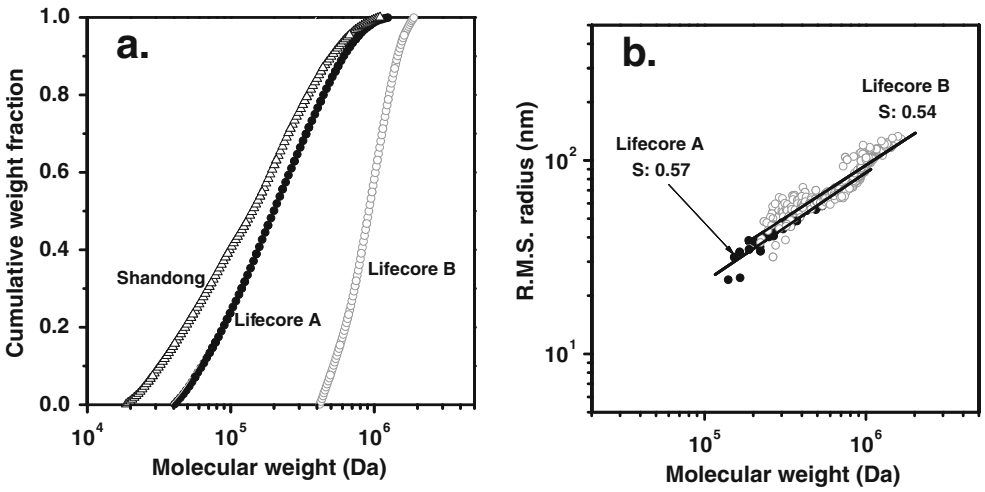

Fig. 2 **a** Cumulative mass distribution curves of commercial NaHA samples and **b** the plot of RMS radius vs. MW

10 min. NaHA and blend mixture samples were dispersed in 0.1 M $NaNO_3$ solution (same as the carrier solution for FlFFF separation) at a concentration of 1.0~1.5 mg/mL and kept in a refrigerator overnight without stirring.

FFF/MALS/DRI

The frit inlet asymmetrical flow field-flow fractionation (FI-AFlFFF) channel that we used in this study had the following channel dimensions: a tip-to-tip length of 27.2 cm, a trapezoidal design with a breadth of 2.0–1.0 cm, and a channel thickness of 178 μm. A PLCGC regenerated cellulose membrane (20 kDa MWCO) from Millipore Corp. (Billerica, MA, USA) was placed above the ceramic frit wall at the accumulation wall. The FI-AFlFFF channel had a small inlet frit (3.0 cm) at the depletion wall through which a high-speed (normally 20 times higher than the sample injection flow rate) flow was introduced to push incoming sample components from the channel inlet toward the accumulation wall, so that hydrodynamic relaxation could be achieved during injection. A FI-AFlFFF channel has the unique feature of hydrodynamic relaxation, and therefore does not require the typical focusing/relaxation procedure that is normally needed for a conventional asymmetrical FlFFF channel.

To separate NaHA and its blend mixtures, programmed field separation was used. This was obtained by decreasing the crossflow rate in a multistep linear decay pattern and the crossflow was circulated to frit flow in such a way that exiting crossflow was connected to the inlet of the frit flow pump via a flow reservoir to damp the pulse from the pump. To deliver the sample and carrier solution to the FI-AFlFFF channel, two HPLC pumps were utilized: a Model 305 HPLC pump from Gilson (Villers Le Bell, France) for sample injection through the sample inlet of the channel and a Model M930 HPLC pump from Young-Lin Co. (Seoul, Korea) for the frit flow through the inlet frit. The carrier solution used for FI-AFlFFF separation was 0.1 M $NaNO_3$, and this solution was filtered by a membrane filter with 0.02 μm pores prior to use. The injection flow rate and the outflow rate to the detector were both 0.1 mL/min. To enable consistent control of the outflow rate, a syringe pump (Model PN1610 Syringe Dosing System from Postnova Analytics, Lansberg, Germany), was utilized in unpump mode at the end of the detector. The two detectors utilized in series were a DAWN-DSP multiangle light scattering detector from Wyatt Technology (Santa Barbara, CA, USA) at a wavelength of 632.8 nm, followed by an Optilab DSP differential refractive index (DRI) detector from Wyatt Technology at a wavelength of 690 nm. Calibration and normalization of MALS were carried out as described in previous reports [24, 25]. The dn/dc value of each sample required for MW calculation was measured with an Optilab DSP refractometer using DNDC5 software from Wyatt. The measured dn/dc values were 0.135 for the HES sample, 0.142 for the raw NaHA sample, 0.141 for the NaHA–HES sample, and 0.138 for the NaHA–NaCMC sample. For the commercial NaHA samples, the dn/dc

Table 1 Calculated weight average (Mw) molecular weight and RMS radius of commercial NaHA products as well as the slope value of the plot of RMS radius vs. MW

	Lifecore A (002799)	Lifecore B (014740)	Shandong HA-TLM
Mw (Da) Manufacturer's	2.34×10^5	7.80×10^5	–
Mw (Da)	$(2.72\pm0.08)\times10^5$	$(9.44\pm0.26)\times10^5$	$(1.91\pm0.16)\times10^5$
Rw (nm)	44.10±0.10	89.60±0.91	39.71±4.01
slope	0.58±0.02	0.55±0.12	0.52±0.10

Table 2 Calculated Mw values of polymer standards obtained using FlFFF-MALS-DRI along with the nominal Mw value for each standard

	Pullulan 400	PSS 350	PSS 1,000
Nominal Mw (Da)	4.00×10^5	3.50×10^5	1.00×10^6
Mw (Da)	$(4.04\pm0.05)\times10^5$	$(3.55\pm0.02)\times10^5$	$(1.01\pm0.01)\times10^6$

values were 0.161 for Lifecore 002799, 0.172 for Lifecore 014740, and 0.150 for the Shandong sample. The dn/dc values of NaHA–HES extracts from NaHA–HES–PLGA film product before and after γ-irradiation were 0.162 for NaHA–HES before irradiation, 0.157 after irradiation at a radiation dose of 15.0 kGy, and 0.142 after irradiation at a dose of 40.0 kGy. For data collection and calculation of MW values, ASTRA software from Wyatt Technology was used. To baseline adjust the DRI signals due to flow programming, we used CORONA software (Wyatt). For MW calculations, polynomial fit according to the Berry method of the Debye plot was utilized for ultralarge MW samples (NaHA–HES for third degree fit, raw NaHA and NaHA-CMC for second degree, Lifecore B for first degree). For other smaller MW samples first degree fit model was used-data points for Lifecore A & NaHA-HES (40 kGy γ-irradiated) were fit under Zimm plot 1st degree exponential, Shandong HATLM & NaHA-HES (15 kGy γ-irradiated) under Zimm plot 1st degree polynomial, and lastly Lifecore B & NaHA-HES (no γ radiation) under Berry plot 1st degree polynomial. These are plotted in the Electronic Supplementary Material Figure S1. LS signals used for the MW calculation were from detector angles of 43°, 52°, 60°, 69°, 80°, 90°, 100°, and 111°.

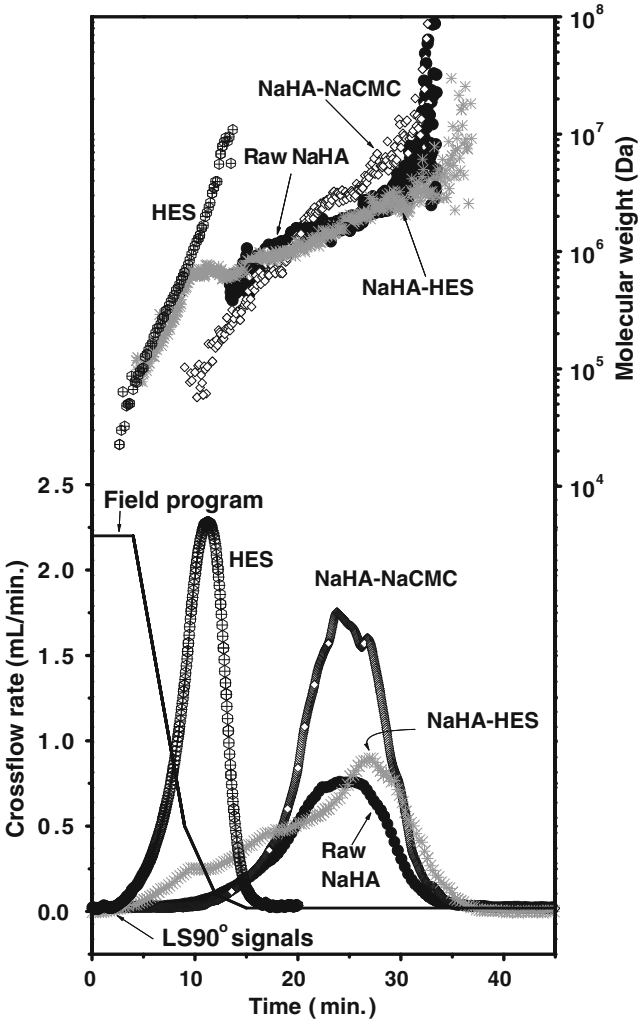

Fig. 3 Fractograms of a HES sample, a raw NaHA product, a NaHA–HES blend mixture, and a commercial anti-adhesive NaHA–NaCMC blend mixture run by FI-AFlFFF-MALS superimposed with calculated MW values. The flow rate conditions were the same as those described in the legend to Fig. 1

Results and discussion

Superimposed fractograms of commercial NaHA samples with different molecular weight distributions are shown in Fig. 1; the calculated MW values at each time slice are plotted above the fractograms. The calculated MW values increased as retention time increased, which indicates that the FI-AFlFFF channel successfully size fractionated NaHA molecules. When calculated MW values of different samples at the same retention time slice overlapped, we interpreted this to mean that the molecular geometries of different samples were similar, because retention in a FI-AFlFFF channel is governed by the hydrodynamic diameter of the sample components. The NaHA products examined in Fig. 1 showed a good overlap between 10^5~10^6 Da, with the exception of a slight difference in the MW region smaller than ~1×10^5 Da. The two Lifecore samples (Mw= 2.34×10^5 Da for A and 7.80×10^5 Da for B) had different elution patterns, resulting in different MWDs. Cumulative MWD curves are superimposed in Fig. 2a, and it is clear that Lifecore sample B had a narrower MW distribution than sample A. Table 1 lists the calculated weight average MW (Mw), number average MW (Mn), polydispersity, and slope of the logarithmic plot of the root-mean-square (RMS) radius (or r_g, radius of gyration) vs. MW, which provides information about the molecular conformation of the sample. The Mw values of the two Lifecore samples were calculated as $(2.72\pm0.08)\times10^5$ and $(9.44\pm0.26)\times10^5$ Da for A and B, respectively, with the latter sample showing a narrower MW distribution, supported by its smaller polydispersity value of 1.09. The Shandong NaHA

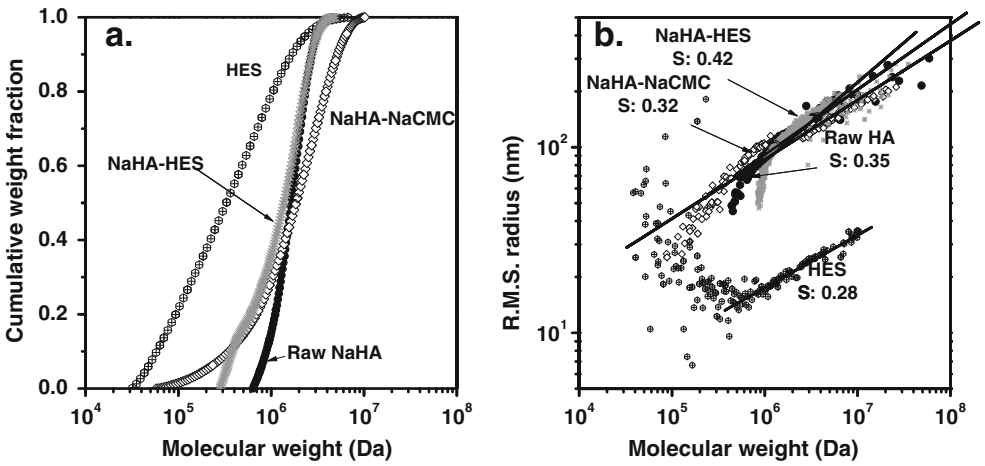

Fig. 4 **a** Comparison of cumulative mass distribution curves of the materials examined in Fig. 3 and **b** the plot of RMS radius vs. MW

sample had a lower Mw value than the Lifecore samples; however, its MW distribution shown in Fig. 2a was much broader than that of the other two samples. The calculated MW values for the two Lifecore samples were somewhat larger than those provided by the manufacturer (A, 2.34×10^5 and B, 7.80×10^5 Da). However, it should be considered that calculated MW values smaller than 100 kDa of Shandong sample may not be accurate due to the poor light scattering signals at low MW region, leading to an overestimation of MW values [29]. Another source of error may arise from the different dn/dc values measured for the commercial NaHA materials. While the known dn/dc value for NaHA is 0.142, the measured values for the commercial samples were 0.161, 0.172, and 0.150 for the two Lifecore's and Shandong sample, respectively. It can be assumed that these materials may contain some different components that can be not separated from pure NaHA materials, which led an error in MW calculation. The performance of the FlFFF-MALS-DRI analysis for the MW calculation employed in this study was tested by running polystyrene sulfonate (PSS) standards, and the calculated Mw values agreed well with the nominal values: $(3.55\pm0.02)\times10^5$ Da for PSS 350 K and $(1.01\pm0.01)\times10^6$ for PSS 1,000 K standards in triplicate measurements. These data are shown in Table 2. Information on the molecular conformation of commercial NaHA samples can be obtained by plotting the RMS radius vs. MW values, as shown in Fig. 2b. The slope values of the two Lifecore samples were 0.57 for sample A and 0.54 for B (values in Table 2 represent each average), indicating that the two Lifecore samples have a linear conformation. For the study of peak recovery, Lifecore B sample was utilized to measure peak area with or without applying crossflow in FlFFF channel. The measured recovery value was 86.6± 4.6% (n=5), which was similar to the reported value (87.2%) with bovine serum albumin [30].

Figure 3 shows superimposed fractograms of a HES (680 kDa) sample, a raw NaHA material used for blending with HES, a NaHA–HES blended sample, and a commercial NaHA–NaCMC mixture sample run under the same flow rate conditions (shown in the figure) by FI-AFlFFF-MALS. The calculated MW values are plotted above the fractograms using a characteristic symbol for each sample. HES molecules eluted with an intense LS peak at 10 min compared to the raw NaHA sample, despite using the same injection amount of 20 μg for both. The calculated MW values of the HES sample increased very smoothly but in a steep way, with an increase in retention time. Furthermore, the HES sample increased in size to a few million Da. Due to the elution of large molecules at early retention time region (<15 min), LS signal of HES can be substantially large compared to the case of smaller MW species eluted at that time interval. However, the cumulative MW distribution plotted in Figure 4a shows that the weight contribution of large molecules (>1 MDa) was less than 20%. While the nominal Mw of the HES sample was 6.80×10^5, the calculated Mw value from experiments was $(6.90\pm0.29)\times10^5$ Da, indicating good agreement. The raw NaHA sample in Fig. 3 has a broad distribution of elution peaks and showed a steady increase in MW values as retention time

Table 3 Calculated Mw, RMS radius, and slope values of RMS radius plot (vs. MW) for the NaHA blend mixture samples and HES

	HES(6.80×10^5 Da)	Raw NaHA	NaHA–HES	commercial NaHA-CMC
Mw (Da)	$(6.90\pm0.29)\times10^5$	$(1.74\pm0.15)\times10^6$	$(1.34\pm0.14)\times10^6$	$(2.58\pm0.09)\times10^6$
Rw (nm)	18.83±2.80	111.60±9.91	97.50±2.43	117.271±2.67
Slope	0.31±0.03	0.36±0.01	0.43±0.01	0.30±0.02

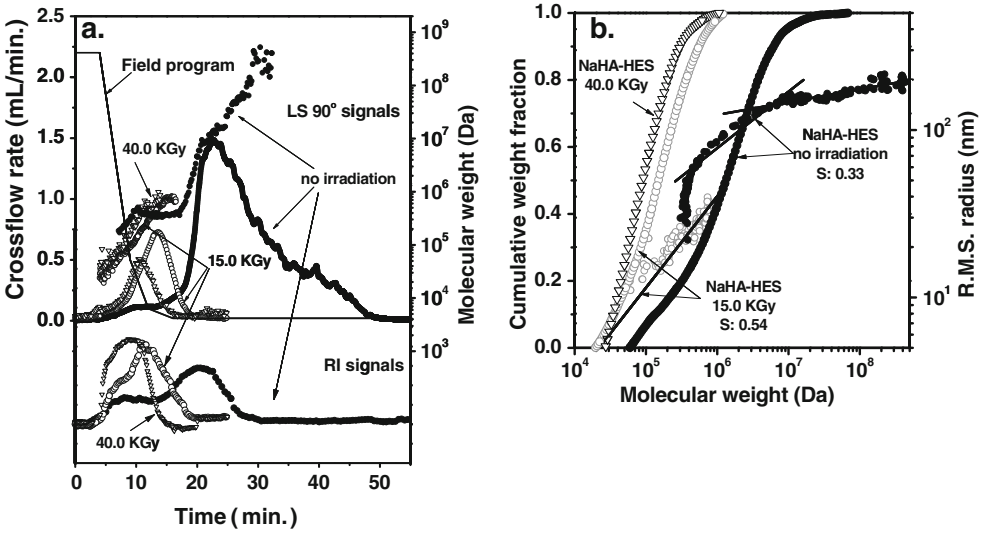

Fig. 5 **a** Fractograms of NaHA–HES extracts from a NaHA–HES–PLGA film product before and after γ-irradiation at two radiation dosages (15.0 and 40.0 kGy) for sterilization and **b** the RMS radius (vs. MW) plot superimposed on the cumulative mass distribution curves

increased, but MW values (black filled circles) increased abruptly after 30 min (~10^7 Da). The NaHA–HES blend mixture sample showed a broader distribution than the raw NaHA sample; the NaHA–HES sample began eluting at 4–5 min with a shoulder at ~10 min, and the entire distribution of MW values spanned up to ~10^7 Da. We hypothesize that this shoulder peak originates from the HES species in the mixture, because calculated MW values at the shoulder peak of the NaHA–HES blended sample (<10 min) matched well with the values obtained for the HES sample. This indicates that HES molecules are not significantly associated with NaHA molecules as complexes or aggregates. The NaHA–HES sample was examined at various field strength conditions but ultrahigh MW species from possible aggregation were not detected. One of the results of the NaHA–HES sample obtained at a different run condition can be found in Electronic Supplementary Material Figure S2 showing that serious formation of aggregates among NaHA molecules with HES did not appear by the calculated MW values at the end of retention and the RMS radius plot vs. MW. The flow rate condition adopted a relatively faster field decay which causes an early elution of large molecules leading to scattered data points at the end of elution. A possible error in MW calculation may arise at or around (10~13 min) the shoulder peak region if molecules of two different geometries but similar hydrodynamic diameter elute together. This coelution could arise from incomplete separation of different components of the blends which can result in an error in the calculation of molecular weight. The evidences of such an incomplete separation can also be found from SEC studies on polymer mixtures [31, 32]. A possibility of which aggregates were lost in channel wall cannot be overlooked. After 12 min, the calculated MW values of the blended mixtures (gray cross) overlapped well with those of the raw NaHA sample (black filled circles) within 12~32 min. This can be explained by the fact that the molecular geometry of the NaHA–HES blend sample did not change much, which is supported by the slope values of the RMS radius plot vs. MW in Fig. 4b: 0.35 and 0.42 for the raw NaHA and the NaHA–HES sample, respectively. When the molecular weight values of HES and NaHA–HES samples (or the raw NaHA sample) were compared, we noted that HES molecules eluted much earlier than NaHA molecules of the same MW. For instance, 1×10^6 Da HES molecules eluted at ~9 min. while the same MW NaHA molecules eluted at ~15 min. Because HES is a branched polymer with a more compact geometry than a linear NaHA molecule, the RMS radius values of HES molecules were much smaller than those of NaHA molecules with the same MW, as shown in Fig. 4b. However, a considerable number of calculated RMS radius values for the HES sample were scattered for MW<4×10^5 Da based on the linear curve. The loss of linearity in the plot of RMS radius vs. MW at the lower MW region of the HES sample was reproducibly observed in our experiments; this may be due to the presence of a less branched molecules. In this case, less branched or relatively linear HES molecules may exhibit a larger RMS radius, which

Table 4 Calculated Mw and RMS radius values of NaHA–HES extracts from NaHA–HES–PLGA film product before and after gamma ray irradiation

	No radiation	15.0 kGy	40.0 kGy
Mw (Da)	$(3.06\pm0.14)\times10^6$	$(2.21\pm0.12)\times10^5$	$(1.49\pm0.09)\times10^5$
Rw (nm)	101.87±8.46	22.60±0.56	27.837±7.77
Slope	0. 34±0.01	0.56±0.02	–

overall results in a distribution of sizes of the same MW. However, molecules larger than ~4×10^5 Da showed a good linear relationship between RMS radius and MW with an average value of 0.31±0.03 (n=3) in Table 3 (0.28 in Fig. 4b), indicating that these molecules have a compact geometry.

In comparison to the NaHA–HES blend, a commercial anti-adhesive NaHA–NaCMC sample showed a unimodal distribution with a broader MW distribution from ~7×10^4 to ~2×10^7 Da (open diamond symbols in Figs. 3 and 4). The calculated MW values of the NaHA–NaCMC sample increased more than those of the NaHA–HES sample in the high MW regime (greater than ~2×10^6 Da). Because the source of NaHA materials used in both samples was different, it is difficult to explain the different patterns seen for the increase in MW values. However, the ultra-large MW region of NaHA molecules underwent a slight change (shrinking) in molecular geometry when they were blended with NaCMC. The RMS radius plots shown in Fig. 4b yielded an average slope value of 0.36±0.01 (n=3) for raw NaHA, 0.43±0.01 (n=3) for NaHA–HES, and 0.30±0.02 (n=3) for NaHA–NaCMC, as listed in Table 3. These values suggest that NaHA molecules may expand to some degree in response to HES; however, they either shrunk or were not affected when exposed to NaCMC molecules.

Figure 5 shows the effects of sterilizing γ-radiation on NaHA–HES–PLGA film products. PLGA, which was added to the NaHA–HES to form a film product, remained as an insoluble particle suspension, and the remaining PLGA particles were removed by ultracentrifugation at 8,550×g for 10 min. A comparison of elution profiles of NaHA–HES samples extracted from a NaHA–HES–PLGA film product before and after γ-radiation at two radiation dosages (15.0 and 40.0 kGy) is shown in Fig. 5a. The fractogram of the NaHA–HES sample not exposed to γ-radiation (Fig. 5a) shows a broader distribution above 30 min than the elution pattern of the NaHA–HES sample in solution shown in Fig. 3. The broader distribution and increase in the larger MW portion of the NaHA–HES sample shown in Fig. 5 was probably caused by aggregation of NaHA molecules during the formation of the film product, showing that the upper MW limit is ~10^8 Da. When the film product was irradiated with γ-rays, the elution peaks of the irradiated NaHA–HES extracts shifted markedly to a shorter time scale, resulting in a significant reduction in the MWD regardless of the radiation dosage. The weight average MW (or Mw) of the NaHA–HES sample decreased from 3.06×10^6 Da to 2.21×10^5 (15 kGy). A comparison of cumulative mass distribution curves superimposed with the RMS radius plot is shown in Fig. 5b. The NaHA–HES sample not exposed to irradiation showed three different slope regimes differentiated by MW values of below ~5×10^5 Da, between 6×10^5–10^7 Da, and above ~10^7 Da. The intermediate MW regime (6×10^5–10^7 Da) had a slope value of 0.33, which is similar to slope value obtained for the raw NaHA and NaHA–HES samples. However, the RMS radius plot for molecules in the ultrahigh MW region (greater than ~10^7 Da) had a flatter slope (~0.1), indicating aggregation. The RMS radius plot for the smaller MW region (<6×10^5 Da) showed a rapid decrease as the MW decreased, reflecting the contribution of HES, which is much smaller than linear molecules. The RMS radius plot of the irradiated sample (15 kGy) revealed that NaHA molecules are broken down by γ-irradiation, resulting in a change in the molecular geometry of the substance from a compact form to a more extended structure (Table 4).

Conclusions

In this study, we used FlFFF-MALS-DRI to characterize NaHA–HES polymer blends both in solution form and in a film product. No significant aggregation between either of the blended mixtures of NaHA with HES or NaCMC was observed on molecular size fractionation and cumulative weight fraction plots. However, we found that gamma radiation caused a serious breakdown of NaHA in a NaHA–HES blended film product. While the difference in gamma radiation dosage (15 vs. 40.0 kGy) did not make a significant difference as shown by molecular size fractionation and cumulative mass distribution plots, both radiation doses decreased the polymer sizes and molecular weights as compared to the untreated control sample.

Acknowledgements This study was supported by a grant from the National Research Foundation of Korea (NRF) funded by the Korea government (MEST) (No.2010-0014046) and in part by NRF grant No. 2011–0001125.

References

1. Iqbal Z, Midgley JM, Watson DG, Karditsas SD, Dutton GN, Wilson W (1997) Pharm World & Sci 19:246–250
2. Yeung B, Marecak D (1999) J Chromatogr A 852:573–581
3. Vercruysse KP, Prestwich GD (1998) Crit Rev Ther Drug Carrier Syst 15:513–555
4. Motohash N, Nakamichi Y, Mori I, Nishijawa H, Umemoto J (1988) J Chromatogr 435:335–342
5. Miyazaki S, Yomota C, Okada S (1996) J Ocul Pharmacol 12:27–34
6. Takahashi R, Al-Assaf S, Williams PA, Kubota K, Okamoto A, Nishinari K (2003) Biomacromolecules 4:404–409
7. Kim JH, Lee JH, Yoon JH, Chang JH, Bae JH, Kim KS (2007) Amer J Rhinology 21:95–99
8. Park WS, Chung YS, Lee KE, Kim HY, Choe JH, Koh SH (2010) Asian J Surgery 33:25–30
9. Cago LA, Saed GM, Chauhan S (2003) Fertil Steril 80:612–616
10. Treib J, Baron JF, Grauer MT, Strauss RG (1999) Intensive Care Med 25:258–268

11. Besheer A, Hause G, Kressler J, Mäder K (2007) Biomacromolecules 8:359–367
12. Mendichi R, Schieroni AG (2002) Polymer 43:6115–6121
13. Giddings JC (1981) Anal Chem 53:1170A–1178A
14. Giddings JC (1993) Science 260:1456–1465
15. Wahlund KG, Giddings JC (1987) Anal Chem 59:1332–1339
16. Ratanathanawongs SK, Giddings JC (1992) Anal Chem 64:6–15
17. Wittgren B, Wahlund KG (1997) J Chromatogr A 760:205–218
18. Wittgren B, Wahlund KG (1997) J Chromatogr A 791:135–149
19. Leeman M, Wahlund KG, Wittgren B (2006) J Chromatogr A 1134:236–245
20. Wittgren B, Borgstorm J, Piculell L, Wahlund KG (1998) Biopolymers 45:85–96
21. Hecker B, Fawell PD, Jefferson A, Farrow JB (1999) J Chromatogr A 837:139–151
22. van Bruijinsvoort M, Wahlund KG, Nilsson G, Kok WT (2001) J Chromatogr A 925:171–182
23. Lee S, Nilsson PO, Nilsson GS, Wahlund KG (2003) J Chromatogr A 1011:111–123
24. Lee H, Kim H, Moon MH (2005) J Chromatogr A 1089:203–210
25. Shin DY, Hwang EJ, Cho IH, Moon MH (2007) J Chromatogr A 1160:270–275
26. Lee H, Cho IH, Moon MH (2006) J Chromatogr A 1131:185–191
27. Moon MH, Shin DY, Lee N, Hwang E, Cho IH (2008) J Chromatogr B 864:15–21
28. Kwon JH, Hwang E, Cho IH, Moon MH (2009) Anal Bioanal Chem 395:519–525
29. Tackx P, Bosscher F (1997) Anal Commun 34:295–297
30. Moon MH, Lee J, Park J (2003) J Liq Chromatogr & Rel Sci 26:2369–2379
31. Gaborieau M, Nicolas J, Save M, Charleux B, Vairon JP, Gilbert RG, Castignolles P (2008) J Chromatogr A 1190:215–233
32. Gaborieau M, Castignolles M (2011) Anal Bioanal Chem 399:1413–1423